# POMERON IN PERTURBATIVE QCD — ITS ELEMENTARY THEORY AND POSSIBLE PHENOMENOLOGY AT HERA*

J. KWIECIŃSKI

Department of Theoretical Physics
H. Niewodniczański Institute of Nuclear Physics
Radzikowskiego 152, 31-342 Cracow, Poland

*(Received March 31, 1992)*

*Dedicated to Wiesław Czyż in honour of his 65th birthday*

Theoretical ideas concerning the Pomeron in perturbative QCD are reviewed. The Lipatov equation with asymptotic freedom effects taken into account is recalled and the corresponding spectrum of eigenvalues controlling the bare Pomeron intercept analysed. Possible phenomenological implications of the perturbative QCD Pomeron for deep inelastic scattering at the HERA ep collider are briefly discussed.

PACS numbers: 12.38.Bx

## 1. Introduction

The name "Pomeron" concerns the mechanism of diffractive processes at high energy. It originated from the Regge pole model developed in the sixties [1]. Within this model one assumes that the dominant mechanism describing the high energy processes is that of the Regge pole exchange (Fig. 1). Formally the Regge pole corresponds to a pole of the partial wave in the crossed $t$-channel in the complex angular momentum plane. Position of this pole is described by the trajectory function $\alpha(t)$. The high energy behaviour of the scattering amplitude corresponding to the Regge pole exchange is :

$$A(s,t) \propto s^{\alpha(t)}, \tag{1.1}$$

* This work has been supported in part by the grant No: 2 0198 91 01 of the Polish Committee of Scientific Research.

where $s$ is the CM energy squared of the colliding particles while $t$ is the square of the four momentum transfer.

Combining (1.1) with the optical theorem one gets the following behaviour of the total cross-section:

$$\sigma_{\text{tot}}(s) \propto s^{\alpha(0)-1}. \tag{1.2}$$

The quantity $\alpha(0)$ is called the intercept. Since, in general, several Regge poles can be exchanged the scattering amplitudes (and the total cross-sections) are given by the sum of terms given by the formulas (1.1) and (1.2) corresponding to exchange of different Regge poles.

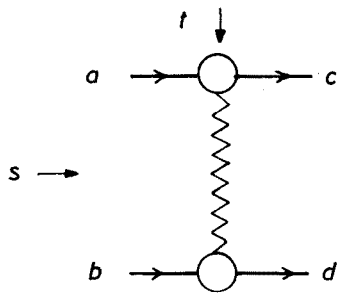


Fig. 1. Regge pole exchange.

The Regge pole exchange is to a large extent the generalization of the one particle exchange. Thus like the ordinary particles also the Regge poles are characterized by the quantum numbers like isospin, $G$-parity *etc.* Being responsible for diffractive scattering Pomeron corresponds, by definition, to the *vacuum* quantum numbers. Other Regge poles carrying quantum numbers different from those of the vacuum are called Reggeons. Within the Regge pole model the Pomeron is a pole having the largest intercept. Historically it has been introduced as the mechanism responsible for the (approximate) energy independence of the total cross-sections that would correspond to $\alpha_{\mathbb{P}}(0) = 1$. It should also be noticed that since the Pomeron corresponds to the vacuum quantum numbers it gives the same total cross-section for particle and antiparticle interactions *i.e.* to the Pomeranchuk theorem which the name "Pomeron" stems from.

The high energy behaviour of scattering amplitudes and so the nature of a Pomeron may be more complicated than that which corresponds to a simple Regge pole exchange picture. In particular the Pomeron should account for the important experimental fact that total cross-sections actually *increase* with the increasing energy [2].

Very important question which is still not entirely understood is the high energy behaviour of elementary processes (and so the Pomeron) in

quantum chromodynamics. This problem is complicated by the fact that the complete description of the high energy behaviour of hadronic processes in QCD is not possible without understanding of colour confinement [3–6]. Much progress has, however, recently been made in understanding the high energy behaviour of elementary processes within perturbative QCD [7–15]. It is believed that the results obtained in this field may be used in the description of the so-called semihard processes where perturbative QCD is expected to be applicable [17–19]. The semihard processes are the hard ones when magnitude of the scale $Q^2$ characterizing the "hardness" of the process is large but much smaller than the total CM energy squared. One of the processes belonging to this class which will be very soon studied in HERA ep collider is the deep inelastic lepton-hadron scattering in the limit $x \cong 0$, where $x$ is the canonical Bjorken $x$ variable (see the formula (2.2) of the next Section).

The purpose of this paper is to review briefly some aspects of the Pomeron physics in *perturbative* QCD. In Sec. 2 we introduce the Lipatov equation for the bare Pomeron. We discuss its properties analysing numerically the spectrum of eigenvalues of the Lipatov kernel in the case when the asymptotic freedom effects are taken into account. The maximal eigenvalue is directly connected with the bare Pomeron intercept. In Sec. 3 we discuss some of the phenomenological implications of the QCD Pomeron in particular for the HERA ep collider. Finally Section 4 contains brief summary and conclusions.

## 2. Lipatov equation and the bare Pomeron in perturbative QCD

When studying the high energy limits of scattering amplitudes in quantum field theories within perturbative approach one usually proceeds in two steps: At first one considers the so-called leading $\log(s)$ approximation. This approximation corresponds to retaining only those terms in the perturbative expansion which give the maximal powers of $\ln(s)$ where $s$ is the CM energy squared of the process. The sum of those terms after projecting on the vacuum quantum numbers in the $t$-channel gives the so called bare Pomeron. The leading $\log(s)$ criterion does not, however, respect unitarity. As the result one finds that in gauge field theories the intercept $\alpha_{\mathrm{P}}^{B}$ of the bare Pomeron is above unity. Since $\sigma_{\mathrm{tot}} \propto s^{\alpha_{\mathrm{P}}^{B}-1}$ this gives the total cross-sections growing as a power of energy with increasing energy. This violates the Froissart bound [18] for sufficiently high energies. In the second step which is in general much more difficult one attempts to understand how the unitarity is restored.

In the non-abelian gauge field theories the leading $\log(s)$ approximation

has been studied in Refs [7–15]. The physical picture of the bare Pomeron is rather simple: it corresponds to the sum of ladder-like diagrams with the exchange of the reggeised gauge bosons (*i.e.* gluons in QCD) along the ladder. In other words the bare Pomeron is given by the multiperipheral production of gauge bosons where the multiperipheral production mechanism is that of the multiregge exchange. Both the gauge vector boson Regge trajectories and the vertices are theoretically calculable. In QCD one may associate the produced gluons with gluon jets. The virtual corrections which lead to the reggeisation of the gluons which are exchanged along the chain can be retranslated into the "non-Sudakov" form-factors [19–22].

In what follows we shall consider the deep inelastic charged lepton--nucleon scattering with its kinematics defined in Fig. 2. In the one-photon approximation this inelastic scattering is related through the one photon exchange mechanism to the virtual photoproduction process induced by the virtual photon. The total cross section of this process is related through the optical theorem to the imaginary part of the forward virtual Compton scattering.

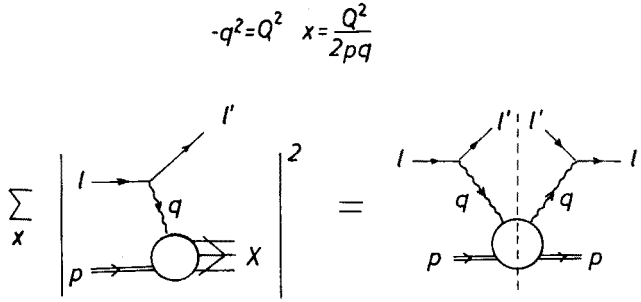


Fig. 2. The kinematics of the deep inelastic scattering and its relation through the optical theorem to the Compton scattering for virtual photons.

We shall consider the virtual Compton scattering in the limit

$$2pq \gg Q^2 \gg \Lambda^2, \tag{2.1}$$

where $\Lambda$ is the QCD scale parameter and $Q^2 = -q^2$ where $q$ is the four momentum transfer between the leptons (see Fig. 2). The limit (2.1) corresponds of course to the high energy limit of the virtual Compton scattering. Important point here is that the magnitude of $Q^2$ is also kept large that will justify the use of perturbative QCD. The limit (2.1) is also equivalent to the small $x$ limit where the Bjorken variable $x$ is defined as:

$$x = \frac{Q^2}{2pq}. \tag{2.2}$$

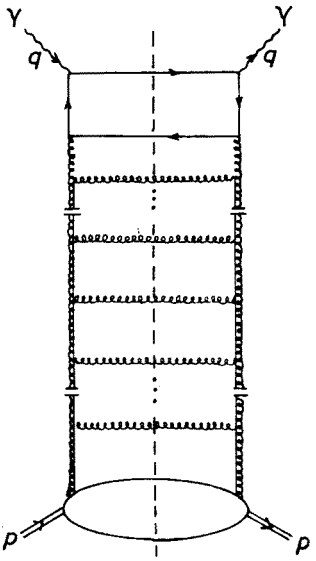


Fig. 3. The ladder diagram for the deep inelastic scattering in the leading $\log(1/x)$ approximation with reggeised gluon exchanges along the chain. The upper part of the diagram corresponds to the sum of the quark box and crossed box of Fig. 4.

In the leading $\log(1/x)$ approximation the structure functions defining the deep inelastic scattering are given by the ladder-like diagrams (Fig. 3) with the reggeised gluon exchange along the ladder. (The leading $\log(1/x)$ approximation is equivalent to the leading $\log(s)$ approximation for the virtual Compton scattering amplitude where $s = (p+q)^2$). In this approximation the small $x$ behaviour of the structure functions is driven by the gluons which couple to the virtual photons through the quark box diagrams (Fig. 4). The fundamental quantity in the leading $\log(1/x)$ approximation is the unintegrated gluon distribution $f(x,k^2)$ related in the following way to the ordinary (scale dependent) gluon distribution $g(x,Q^2)$:

$$f(x,k^2) = \left.\frac{\partial x g(x,Q^2)}{\partial \ln Q^2}\right|_{Q^2=k^2}. \tag{2.3}$$

The deep inelastic structure function $F_2(x,Q^2)$ is related to this function through the following formula:

$$F_2(x,Q^2) = \int_x^1 \frac{dx'}{x'} \int_0^\infty \frac{dk^2}{k^2} F_{2g}(x',k^2,Q^2) f\left(\frac{x}{x'},k^2\right), \tag{2.4}$$

where the function $F_{2g}(x', k^2, Q^2)$ is the (suitably defined) gluon structure function corresponding to the sum of quark box diagrams of Fig. 4. The formula (2.4) is an example of the "$k_t$ factorization theorem" [23] ($k \equiv k_t$ where $k_t$ is the transverse momentum of the gluon). The physical content of this theorem is that the cross-sections of semihard processes in the leading $\log(s)$ (or $\log(1/x)$) approximation can be expressed as the (double) convolution in the transverse and longitudinal momenta of the universal (unintegrated) gluon distribution and the corresponding hard cross sections on the partonic level. The small $x$ behaviour is entirely driven by the unintegrated gluon distribution.

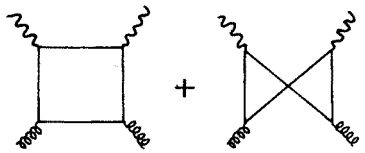

Fig. 4. The two diagrams describing the gluon-photon interaction. The internal lines correspond to quarks.

In the leading $\log(1/x)$ approximation the formula (2.4) simplifies to give:

$$F_2(x, Q^2) = \int_0^\infty \frac{dk^2}{k^2} \Phi_{2g}^{(0)}(k^2, Q^2) f(x, k^2) \tag{2.5}$$

with the "impact factor" $\Phi_{2g}^{(0)}(k^2, Q^2)$ defined by:

$$\Phi_{2g}^{(0)}(k^2, Q^2) = \int_0^1 \frac{dx'}{x'} F_{2g}(x', k^2, Q^2). \tag{2.6}$$

The ladder-like iteration gives the Lipatov equation for the unintegrated gluon distribution $f(x, k^2)$ [7–17,19–23]:

$$f(x, k^2) = f_0(k^2) + \frac{3\alpha_s}{\pi} k^2 \int_x^1 \frac{dx'}{x'} \int_0^\infty \frac{dk'^2}{k'^2} \times \left( \frac{f(x', k'^2) - f(x', k^2)}{| k'^2 - k^2 |} + \frac{f(x', k^2)}{(k^4 + 4k'^4)^{1/2}} \right). \tag{2.7}$$

In this equation $k^2(k'^2)$ are the transverse momenta squared of the gluons, $\alpha_s$ is the strong interaction coupling and $f_0(k^2)$ is the suitably defined

inhomogeneous term. In order to study this equation it is convenient to use the moment $\bar{f}(n,k^2)$ of the function $f(x,k^2)$ defined as below:

$$\bar{f}(n,k^2) = \int_0^1 dx x^{n-2} f(x,k^2) \tag{2.8}$$

which satisfies the following equation:

$$\begin{aligned}\bar{f}(n,k^2) =& \frac{f_0(k^2)}{(n-1)} + \frac{3\alpha_s}{\pi(n-1)} k^2 \int_0^\infty \frac{dk'^2}{k'^2} \\ & \times \left( \frac{\bar{f}(n,k'^2) - \bar{f}(n,k^2)}{|\, k'^2 - k^2 \,|} + \frac{\bar{f}(n,k^2)}{(k^4 + 4k'^4)^{1/2}} \right) \\ =& \frac{f_0(k^2)}{(n-1)} + \frac{1}{(n-1)} K_L \otimes \bar{f}. \end{aligned} \tag{2.9}$$

The leading singularity $n_L$ of $f(n,k^2)$ in the $n$-plane controls the small $x$ limit of the gluon distribution $f(x,k^2)$. This leading singularity is given by the maximal eigenvalue $\lambda_{max}$ of the Lipatov kernel $K_L$ *i.e.*:

$$n_L = 1 + \lambda_{max} \tag{2.10}$$

with $\lambda_{max}$ given by the following formula:

$$\lambda_{max} = \frac{12 \ln(2) \alpha_s}{\pi}. \tag{2.11}$$

The formulas (2.10) and (2.11) give the intercept of the bare Pomeron *i.e.* $\alpha_P^B = n_L$. A simple explanation of the relation between the maximal eigenvalue of the Lipatov kernel and the bare Pomeron intercept is given in Ref. [24]. It can have potentially large magnitude $\alpha_P^B > 1.5$ or so. This bare Pomeron controls the small $x$-behaviour of the gluon distribution $f(x,k^2)$ *i.e.*:

$$f(x,k^2) \propto \frac{x^{1-\alpha_P^B}}{[\ln(1/x)]^{1/2}} \left( 1 + O\left( \frac{1}{\ln(1/x)} \right) \right). \tag{2.12}$$

The relatively unimportant factor $1/[\ln(1/x)]^{1/2}$ comes from the fact that the spectrum of the Lipatov kernel is continuous.

Although the Lipatov equation is free from infrared singularities at $k^2 = 0$ one does not expect that the region of low $k^2$ where the confinement effects are important is treated reliably. The possible way of incorporating the non-perturbative effects in the Lipatov equation has been discussed in Ref. [25].

Moreover in the large $k^2$ region the asymptotic freedom effects should be included.

The simplest way to eliminate the low $k^2$ region is to impose the lower limit cut-off $k_0^2$ in the integrals in Eqs (2.7) and (2.9). The asymptotic freedom effects can be taken into account substituting the running QCD coupling $\alpha_s(k^2)$ in place of the fixed (*i.e.* $k^2$ independent) coupling $\alpha_s$. The Lipatov equation then reads:

$$\begin{aligned}\bar{f}(n,k^2) =& \frac{f_0(k^2)}{(n-1)} + \frac{3\alpha_s(k^2)}{\pi(n-1)} k^2 \int_{k_0^2}^{\infty} \frac{dk'^2}{k'^2} \\ & \times \left( \frac{\bar{f}(n,k'^2) - \bar{f}(n,k^2)}{|\, k'^2 - k^2 \,|} + \frac{\bar{f}(n,k^2)}{(k^4 + 4k'^4)^{1/2}} \right) \\ =& \frac{f_0(k^2)}{(n-1)} + \frac{1}{(n-1)} \bar{K}_L(k_0^2) \otimes \bar{f}. \end{aligned} \tag{2.13}$$

The spectrum of the kernel $\bar{K}_L(k_0^2)$ is now discrete. The maximal eigenvalue can be shown to satisfy the following inequality [26]:

$$3.6 \frac{\alpha_s(k_0^2)}{\pi} < \lambda_{\max} < 12 \ln(2) \frac{\alpha_s(k_0^2)}{\pi}. \tag{2.14}$$

The most recent discussion of the Lipatov equation is presented in Ref. [27].

Eq. (2.7) is also modified accordingly *i.e.*:

$$\begin{aligned} f(x,k^2) = f_0(k^2) + \frac{3\alpha_s(k^2)}{\pi} k^2 \int_x^1 \frac{dx'}{x'} \int_{k_0^2}^{\infty} \frac{dk'^2}{k'^2} \\ \times \left( \frac{f(x',k'^2) - f(x',k^2)}{|\, k'^2 - k^2 \,|} + \frac{f(x',k^2)}{(k^4 + 4k'^4)^{1/2}} \right). \end{aligned} \tag{2.15}$$

This equation has been studied numerically in Refs [28–31]. It turns out that the effective $x^{-\lambda}$ behaviour emerges relatively soon in the solution of this equation with $\lambda$ being dependent upon cut-off $k_0^2$ [30,31]. The magnitude of $\lambda$ is still relatively large (*i.e.* $< 0.5$ or so).

The solution of the Eq. (2.15) contains contributions of all eigenvalues particularly in the region of moderately small values of $x$. It may therefore be interesting to analyse the distribution of eigenvalues. To this aim we have analysed the spectrum of the kernel $\bar{K}_L(k_0^2)$ suitably adapting the numerical methods used in [28–31] where the solution of the Lipatov equation was approximated by the truncated series of the Tchebyshev polynomials linear

in $\ln(k^2)$. (We also impose upper limit cut-off but the results are very insensitive to its magnitude.) In this way the problem is reduced to finding the eigenvalues of the (finite order) matrix constructed from the kernel $\bar{K}_{\mathrm{L}}(k_0^2)$. The distribution of eigenvalues (for $k_0^2 = 2\ \mathrm{GeV}^2$) is presented in Fig. 5. It may be seen that the leading eigenvalue is very well separated from the non-leading ones. This may explain the relatively rapid onset of the simple power-law behaviour found in [30,31]. In Fig. 6 we illustrate the cut-off dependence of the leading eigenvalue $\lambda_{\max}$ where we plot its inverse with respect to $\ln(k_0^2/\Lambda^2)$. We find approximate linear dependence suggesting that $\lambda_{\max} \propto \alpha_s(\beta k_0^2)$. From Fig. 6 one finds $\lambda_{\max} \cong 1.84 \cdot 3\alpha_s(9.16 k_0^2)/\pi$. This should be compared with the fixed coupling case (2.11) which gives $\lambda_{\max} \cong 2.77 \cdot 3\alpha_s/\pi$.

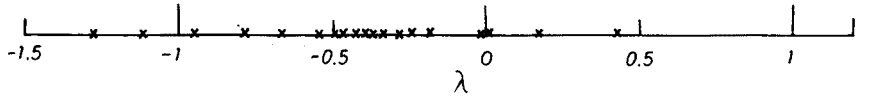


Fig. 5. Distribution of eigenvalues of the Lipatov kernel $\bar{K}_{\mathrm{L}}(k_0^2)$ for $k_0^2 = 2\ \mathrm{GeV}^2$.

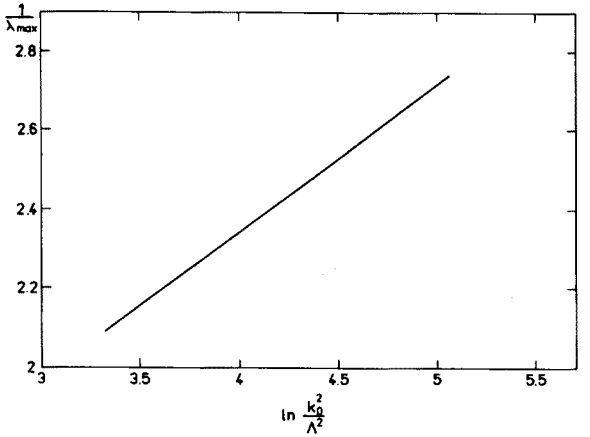


Fig. 6. The cut-off dependence of the leading eigenvalue $\lambda_{\max}$ of the Lipatov kernel $\bar{K}_{\mathrm{L}}(k_0^2)$.

For the very small values of $x$ the indefinite increase of the gluon distributions enhances the probability of gluon fusion and recombination. This interaction of small $x$ partons leads to screening effects which modify the

Lipatov equation in the following way [15,31]:

$$f(x,k^2) = f_0(k^2) + \frac{3\alpha_s(k^2)}{\pi}k^2 \int_x^1 \frac{dx'}{x'} \int_{k_0^2}^{\infty} \frac{dk'^2}{k'^2}$$
$$\times \left( \frac{f(x',k'^2) - f(x',k^2)}{|\, k'^2 - k^2 \,|} + \frac{f(x',k^2)}{(k^4 + 4k'^4)^{1/2}} \right)$$
$$- \frac{81\alpha_s^2(k^2)}{16R^2k^2} \int_x^1 \frac{dx'}{x'} \left(x'g(x',k^2)\right)^2. \qquad (2.16)$$

The screening effects are given by the last term in the Eq. (2.16) where the parameter $R$ corresponds to the (transverse) size of the region within which the partons (*i.e.* gluons) are concentrated.

Eq. (2.16) goes of course beyond the leading $\log(1/x)$ approximation. It is in fact an example of the unitarization procedure on the parton distribution level. The negative screening term tames the indefinite increase of parton distributions in the small $x$ region turning it into (approximately) $x$ -independent saturation limit. To be precise the Eq. (2.16) generates in a self-consistent way the $x^{-\lambda}$ behaviour and simultaneous taming of this behaviour by the non-linear screening term. Its detailed analysis is presented in Ref. [31].

More conventional way to introduce parton screening effects is to include them in the standard QCD evolution formalism [24,32]. An implementation of both the singular $x^{-\lambda}$ behaviour and screening effects within this formalism was done in [24] and will be very briefly discussed in the next Section.

## 3. Possible phenomenological implications of the perturbative QCD Pomeron

In the previous Section we have discussed the bare Pomeron in perturbative QCD concentrating on the small $x$ limit of gluon distribution in a hadron. The Pomeron singularity which corresponds to the exchange of the gluon ladders diagram is of course universal and should manifest itself in any elementary process in which the exchange of the vacuum quantum numbers are possible. The process should also be "hard" *i.e.* it should involve some large scale "$Q^2$" for perturbative QCD to be applicable.

The deep inelastic lepton scattering in the limit of small $x$ is the possible "hard" process where the effects of the perturbative QCD Pomeron should show up. The perturbative QCD analysis of the parton distributions

in a nucleon which incorporated both the QCD Pomeron as well as parton screening was performed in Ref. [24]. The QCD Pomeron effects were included using the singular parametrization (*i.e.* proportional to $x^{-\lambda}$ with $\lambda = {}^1/_2$) of gluon and sea quark input distributions at the reference scale $Q_0^2 = 4$ GeV$^2$. We label this parametrization as $B_-$. The parton screening was next included by suitably modifying this input parametrization and by adding the non-linear terms in the evolution equations like the last term in the Eq. (2.16). The screening effects were considered for $R = 2$ GeV$^{-1}$ and $R = 5$ GeV$^{-1}$. In Fig. 7 we show the results of this analysis for the structure function $F_2$ in the region of small $x$ which will be soon probed by the HERA collider. For comparison the result corresponding to the $B_0$ set of parton distributions based on the non-singular input is also shown.

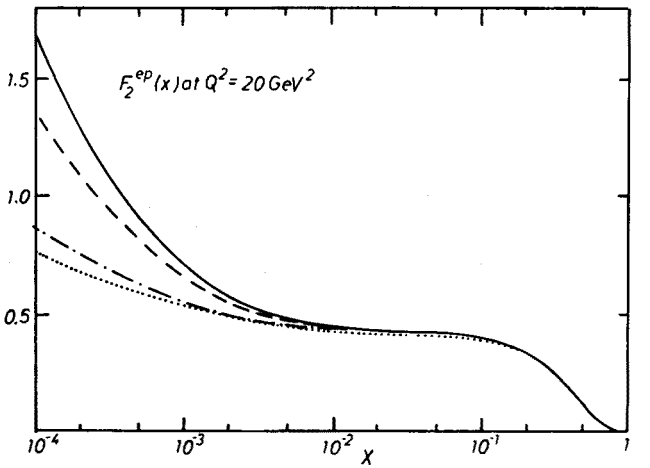


Fig. 7. The structure function $F_2^{ep}$ as a function of $x$ at $Q^2 = 20$ GeV$^2$. The solid line corresponds to the $B_-$ set of parton distributions. The dashed and dot-dashed lines indicate the correction due to parton screening effects with $R = 5$ GeV$^{-1}$ and 2 GeV$^{-1}$ respectively. For comparison the prediction from the $B_0$ set of partons is shown by the dotted curve. (Results of this analysis were taken from Ref. [24]).

Presumably the ideal process which may test the perturbative QCD Pomeron most directly is the jet production in deep inelastic scattering in the small $x$ region [33–36]. The kinematics of the jet should be such that $x_{\rm jet} \gg x$ and $k^2 \cong Q^2$, where $k$ is the jet transverse momentum. The jet production in this configuration is expected to be described by the diagrams of Fig. 8. The upper part of this diagram corresponds just to the (bare) QCD Pomeron. Important point here is that it can be computed entirely within perturbative QCD including its normalization which is controlled by the sum of quark box (and crossed box) diagrams contribution to the virtual photon-gluon interaction (see Fig. 4). By choosing the configuration $k^2 \cong Q^2$ it is possible to eliminate the effect of the ordinary QCD evolution

(from the scale $k^2$ to $Q^2$) in which transverse momenta are ordered along the chain. In this configuration one is therefore able to test directly the complete ladder equation in which the transverse momenta are not ordered. The detailed theoretical analysis of this process has recently been performed in Refs [35,36].

The differential structure function $x_j \partial F_2(x, Q^2; x_j, k^2)/\partial x_j \partial k^2$ describing the jet production is given by the following formula [36]:

$$x_j \frac{\partial F_2(x, Q^2; x_j, k^2)}{\partial x_j \partial k^2} = \frac{3\alpha_s(k^2)}{\pi k^4} \left( \sum_a x_j f_a(x_j, k^2) F\left(\frac{x}{x_j}, k^2, Q^2\right) \right), \tag{3.1}$$

where the sum over parton distributions in a nucleon is:

$$\sum_a f_a = g + \frac{4}{9}(q + \bar{q}). \tag{3.2}$$

The function $F$ satisfies the Lipatov equation suitably adapted to the kinematics of Fig. 8 [36].

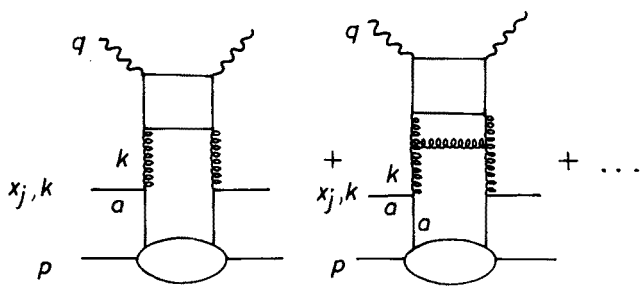


Fig. 8. The leading $\log(x_j/x)$ approximation to the deep inelastic scattering containing an identified jet of longitudinal and transverse momentum $x_j p$ and $k$ respectively. The upper part of the diagram corresponds to the sum of the quark box and crossed box of Fig. 4.

In Fig. 9 we present the prediction for the differential structure function $x_j \partial F_2(x, Q^2; x_j, k^2)/\partial x_j \partial k^2$ obtained in Ref. [36]. For comparison we also show the case when the ladder effects are neglected. In this approximation one sets in the Eq. (3.1) in place of the function $F(x/x_j, k^2, Q^2)$ the $x/x_j$ independent impact factor $F_0(k^2, Q^2)$ corresponding to the sum of quark box and crossed box diagrams. It may be seen from this Figure that the QCD Pomeron significantly modifies the jet spectrum. Measurement of jet

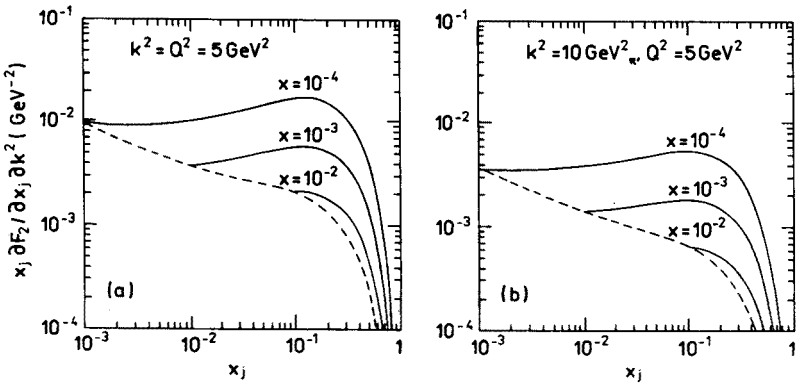


Fig. 9. The differential structure function for deep inelastic $(x, Q^2)$ events with an identified jet $(x_j, k^2)$ as a function of $x_j$ for different values of $x$, $x = 10^{-4}, 10^{-3}$ and $10^{-2}$, and for $Q^2 = 5$ GeV$^2$. The dashed curve is obtained from (3.1) with $F$ replaced by the driving term $F_0$ corresponding to the quark box diagram contribution alone. The magnitude of the cut-off defining $F_0$ as well as the magnitude of the cut-off $k_0^2$ in the Lipatov equation is chosen to be equal to 1 GeV$^2$. Figures (a) and (b) correspond to the jet transverse momentum squared $k^2 = 5$ and 10 GeV$^2$ respectively. (Results of this analysis were taken from Ref. [36]).

production in deep inelastic scattering should in principle be possible at HERA.

The perturbative QCD Pomeron should also affect the heavy quark production and the detailed analysis of this problem is presented in Ref. [23].

Important process which may test the partonic content of a Pomeron (and so its underlying QCD structure) is diffractive production in deep inelastic lepton scattering *i.e.* the process: $\gamma^*(Q^2) + p \Rightarrow X + p$ with large rapidity gap between the proton in a final state and the hadronic system $X$ [37–40]. The diffractive production in inelastic lepton scattering controls also the nuclear shadowing effects in deep inelastic lepton scattering on nuclei at small $x$ [41–43]. The partonic content of a Pomeron can also be revealed in studying the jet production within the diffractively produced system in hadronic collisions [44,45].

The QCD Pomeron should also manifest itself in total cross-sections in hadronic collisions. The natural component of the total cross section which can be associated with the QCD Pomeron is that which corresponds to the mini-jet production [46,47].

## 4. Summary and conclusions

In this paper we have reviewed some of the problems concerning the Pomeron in perturbative QCD. We have discussed with some detail the so

called bare Pomeron which emerges from the study of the high energy limit of elementary processes in QCD in the leading $\log(s)$ approximation. In deep inelastic scattering this approximation becomes the leading $\log(1/x)$ approximation where $x$ is the canonical Bjorken $x$ variable. The main contribution in the small $x$ limit of the deep inelastic scattering comes from the sea quarks and antiquarks which are driven by the gluons. In the leading $\log(1/x)$ approximation the gluon distributions are given by ladder-like diagrams with the reggeised gluon exchange along the chain. The sum of these ladder diagrams gives the Lipatov equation which generates the bare QCD Pomeron. We have briefly analysed the eigenvalue spectrum of the Lipatov equation kernel with the asymptotic freedom effects taken into account. In the small $x$ limit the parton distributions (multiplied by $x$) have the $x^{-\lambda}$ behaviour where $\lambda$ is equal to the maximal eigenvalue $\lambda_{\max}$. The bare Pomeron intercept $\alpha_{\mathrm{P}}^{B}$ is equal to $1 + \lambda_{\max}$. The unique feature of the QCD Pomeron is potentially large magnitude of its intercept $\alpha_B^P \cong 1.5$. We have also briefly mentioned the parton screening effects which bring the bare Pomeron within the unitarity limits. More detailed discussion of these effects is given in Refs [16,17,24,31,32,48].

The choice of problems presented in this paper has been very selective and we decided to discuss those aspects of the perturbative QCD Pomeron physics which can be directly accessible to experimental verification particularly at the HERA ep collider. Our discussion focussed entirely on the Pomeron at $t = 0$. In particular we have entirely omitted important issues concerning shrinkage patterns of the diffractive peak. These problems are discussed in detail in Ref. [48]. Moreover our discussion concerned only properties of the *perturbative* Pomeron. Possible non-perturbative effects which take into account non-perturbative modifications of the gluon propagators coming from the gluon condensate are discussed in Refs [4–6,25].

In Sec. 3 we discussed some of the experimental measurements which can reveal the properties of the QCD Pomeron. The measurement of jet production in deep inelastic lepton scattering at HERA in the kinematical configuration $x_j \gg x$ and $k^2 \cong Q^2$ will presumably be the "landmark" measurement in this respect.

I am most grateful to Barbara Badełek, Krzysztof Charchuła, Krzysztof Golec-Biernat, Maria Krawczyk, Alan Martin, Dick Roberts, James Stirling, Dorota Strózik-Kotlorz and Peter Sutton for numerous discussions and for very enjoyable collaboration on some of the problems discussed in this paper.

**Note added in proof:** After this paper had been completed I became aware of the new structure function analysis performed in the Ref. [50] which included the most recent NMC data [51]. The results of this analysis differ from those obtained in the Ref. [24] and summarised in Fig. 7.

## REFERENCES


[1] P.D.B. Collins, *An introduction to Regge theory and high energy physics*, Cambridge University Press, Cambridge, 1977.

[2] R. Castaldi, G. Sanguinetti, *Annu. Rev. Nucl. Part. Sci.*, **35**, 351 (1985); J.G. Rushbrooke, in *Proceedings of the International Europhysics Conference on High Energy Physics*, Bari Italy, 1985, Eds L. Nitti, G. Preparata Laterza, Bari, 1985; E710 Collaboration; N.A. Amos *et al.*, *Phys. Rev. Lett.* **63**, 2784 (1989); *Phys. Lett.* **B243** 158 (1990); *Phys. Lett.* **B247**, 127 (1990).

[3] A.R. White, Argonne Nat. Lab. preprints: ANL-HEP-PR-87-92, ANL-HEP-PR-87-68, ANL-HEP-PR-89-18, ANL-HEP-PR-89-104; *Int. J. Mod. Phys.* **A6**, 1859 (1991).

[4] P.V. Landshoff, O. Nachtmann, *Z.Phys.* **C35**, 405 (1987).

[5] J.R. Cudell, A. Donnachie, P.V. Landshoff, *Nucl. Phys.* **B322**, 55 (1989).

[6] A. Donnachie, P.V. Landshoff, *Nucl. Phys.* **B311**, 509 (1989).

[7] E.A. Kuraev, L.N. Lipatov, V.S. Fadin, *Zh. Eksp. Teor. Fiz.* **72**, 373 (1977) 373, *Sov. Phys. JETP* **45**, 373 (1977).

[8] J.B. Bronzan, R.L. Sugar, *Phys. Rev.* **D17**, 585 (1978).

[9] Ya.Ya. Balitzkij, L.N. Lipatov, *Yad. Fiz.* **28**, 1597 (1978).

[10] A.R. White, *Nucl. Phys.* **B151**, 77 (1979).

[11] J. Bartels, *Nucl. Phys.* **B151**, 293 (1979) 293; *Acta Phys. Pol.* **B11**, 281 (1980).

[12] T. Jaroszewicz, *Acta Phys. Pol.* **B11**, 965 (1980).

[13] L.N. Lipatov, *Sov. Physics JETP* **63**, 904 (1986).

[14] L.N. Lipatov, in *Perturbative QCD*, World Scientific, ed. A.H. Mueller, 1989, p. 411.

[15] L.N. Gribov, E.M. Levin, M.G. Ryskin, *Phys. Rep.* **100**, 1 (1983).

[16] E.M. Levin, M.G. Ryskin, *Phys. Rep.* **189**, 267 (1990).

[17] B. Badełek, K. Charchuła, M. Krawczyk, J. Kwieciński, DESY preprint, DESY-91-124.

[18] M. Froissart, *Phys. Rev.* **123**, 1053 (1961); A. Martin, *Z. Phys.* **C15**, 185 (1982).

[19] M. Ciafaloni, *Nucl. Phys.* **B296**, 49 (1988).

[20] G. Marchesini, B.R. Webber, *Nucl. Phys.* **B349**, 617 (1991).

[21] S. Catani, F. Fiorani, G. Marchesini, *Phys. Lett.* **B234**, 339 (1990); *Nucl. Phys.* **B336**, 18 (1990).

[22] E.M. Levin, G. Marchesini, M.G. Ryskin, B.R. Webber, *Nucl. Phys.* **B357**, 167 (1991).

[23] S. Catani, M. Ciafaloni, F. Hautman, *Phys. Lett.* **B242**, 97 (1990); *Nucl. Phys.* **B366**, 135 (1991); J.C. Collins, R.K. Ellis, *Nucl. Phys.* **B360**, 3 (1991).

[24] J. Kwieciński, A.D. Martin, W.J. Stirling, R.G. Roberts, *Phys. Rev.* **D42**, 3645 (1990).

[25] D.A. Ross, *J. Phys. G* **15**, 1175 (1989).

[26] J.C. Collins, J. Kwieciński, *Nucl. Phys.* **B316**, 307 (1989).

[27] J.C. Collins, P.V. Landshoff, *Phys. Lett.* **B276**, 196 (1992).

[28] J.Kwieciński, *Z. Phys.* **C29**, 561 (1985).

[29] K.Charchuła, M.Krawczyk, DESY preprint, DESY-90-122; M. Krawczyk, *Nucl. Phys. (Proc. Suppl.)* **B18**, C64 (1990).
[30] D. Strózik-Kotlorz, *Z. Phys.* **C53**, 493 (1992).
[31] J. Kwieciński, A.D. Martin, P.J. Sutton, *Phys. Lett.* **B264**, 199 (1991); *Phys. Rev.* **D44**, 2640 (1991).
[32] A.H. Mueller, J. Qiu, *Nucl. Phys.* **B268**, 427 (1986).
[33] A.H. Mueller, *Nucl. Phys. (Proc. Suppl.)* **B18**, C125 (1990); *J. Phys. G* **17**, 1443 (1991).
[34] J. Bartels, *Particle World*, **2**, 46 (1991).
[35] J. Bartels, A. de Roeck, M. Loewe, DESY preprint, DESY-91-154.
[36] J. Kwieciński, A.D. Martin, P.J. Sutton, Durham Univ. preprint DTP/92/04.
[37] A. Donnachie, P.V. Landshoff, *Nucl. Phys.* **B244**, 322 (1984); *Phys. Lett.* **B191**, 309 (1987).
[38] J. Bartels, G. Ingelman, *Phys. Lett.* **B235**, 175 (1990); G. Ingelman , *Nucl. Phys. B (Proc. Suppl.)* **18C**, 55 (1990).
[39] M.G. Ryskin, *Sov. Journ. Nucl. Phys.* **47**, 230 (1988); DESY preprint, DESY-90-150.
[40] N.N. Nikolaev, B.G. Zakharov, Torino Univ. preprint DFTT-5/91.
[41] B. Badełek, J. Kwieciński, *Phys. Lett.* **B208**, 508 (1988); *Nucl. Phys.* **B370**, 278 (1992); J. Kwieciński, *Z. Phys.* **C45**, 461 (1990).
[42] N.N. Nikolaev, B.G. Zakharov, *Z. Phys.* **C49**, 607 (1991).
[43] V.R. Zoller, ITEP preprints 58-91, 102-91.
[44] G. Ingelman, P.E. Schlein, *Phys. Lett.* **B152**, 256 (1985).
[45] E.L. Berger, J.C. Collins, D.E. Sopper, G. Sterman, *Nucl. Phys.* **B286**, 704 (1987).
[46] J. Kwieciński, *Phys. Lett.* **B187**, 386 (1987); A. Capella, J. Tran Thanh Van, J. Kwieciński, *Phys. Rev. Lett.* **58**, 2015 (1987).
[47] L. Durand, H. Pi, *Phys. Rev. Lett.* **58**, 303 (1987); *Phys. Rev.* **D38**, 78 (1987); ibid. **D40**, 1436 (1989).
[48] J. Bartels, J. Blümlein, G. Schuler, *Z. Phys.* **C50**, 91 (1991).
[49] E.M. Levin, M.G. Ryskin, *Sov. J. Nucl. Phys.* **50**, 881 (1989); *Z. Phys.* **C48**, 231 (1990); M.G. Ryskin, *Nucl. Phys. B (Proc. Suppl.)* **12**, 40 (1990).
[50] A.D. Martin, W.J. Stirling, R.G. Roberts, Univ. of Durham preprint DTP/92/16 (RAL-92-021).
[51] E. Kabuss, invited talk at DESY-Zeuthen Workshop on Deep Inelastic Scattering, April 1992.